

Supplementary Materials for

Extracellular matrix stiffness determines DNA repair efficiency and cellular sensitivity to genotoxic agents

Min Deng*, Jing Lin, Somaira Newsheen, Tongzheng Liu, Yingchun Zhao, Peter W. Villalta, Delphine Sicard, Daniel J. Tschumperlin, SeungBaek Lee, JungJin Kim, Zhenkun Lou*

*Corresponding author. Email: deng.min@mayo.edu (M.D.); lou.zhenkun@mayo.edu (Z.L.)

Published 11 September 2020, *Sci. Adv.* **6**, eabb2630 (2020)
DOI: [10.1126/sciadv.abb2630](https://doi.org/10.1126/sciadv.abb2630)

This PDF file includes:

Figs. S1 to S9

Figure S1

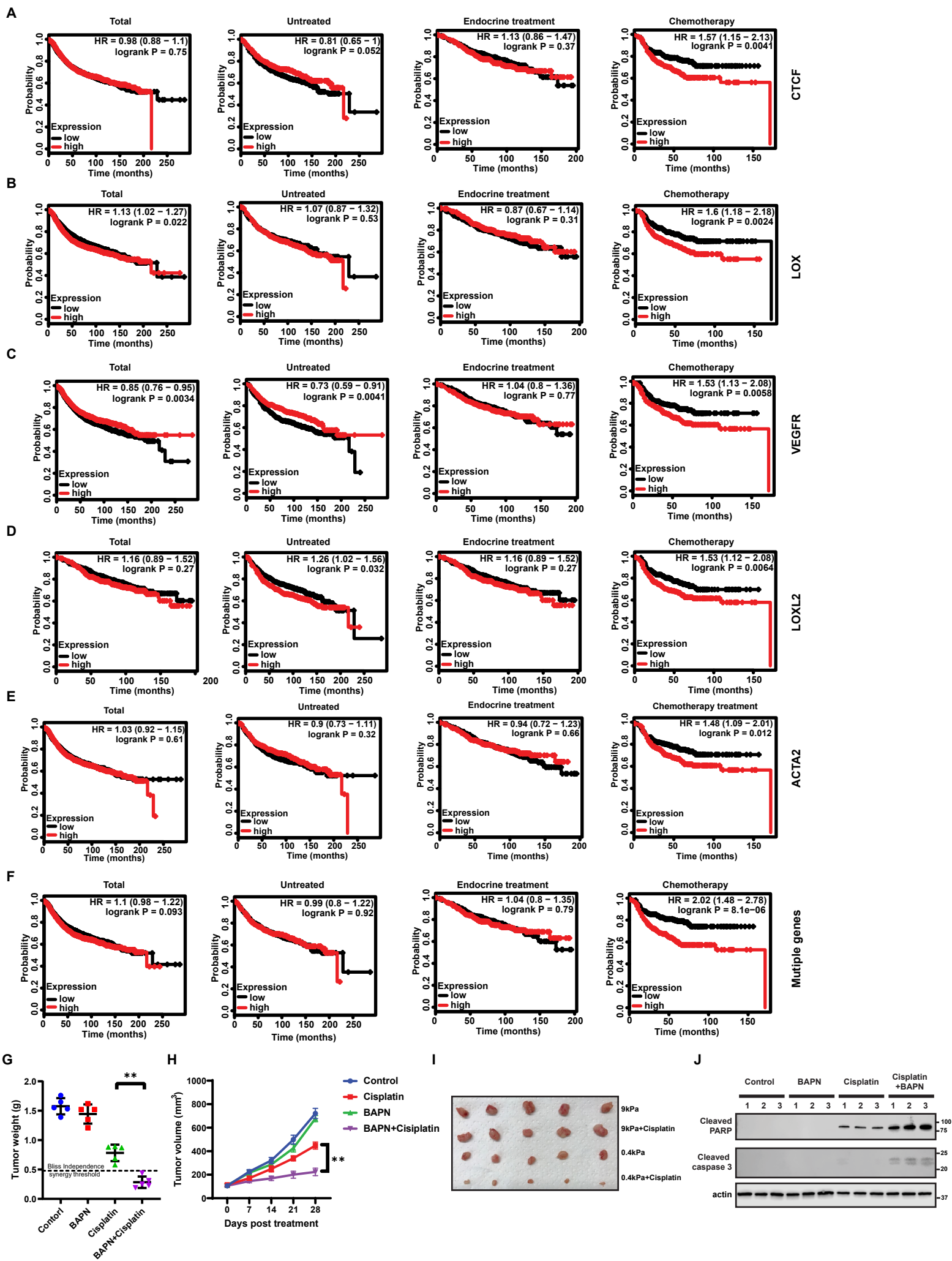


Fig.S1 ECM stiffness regulates tumor chemo-sensitivity.

(A to F) Survival for stiffness marker genes with different treatments in breast cancer patients. Kaplan-Meier survival plots show that higher expression of CTGF (A), LOX (B), VEGFR (C), LOXL2 (D) and ACTA2 (E) results in a worse survival after chemotherapy treatment while has subtle effect when untreated or endocrine treatment was used. Combination of these genes (F) has similar effect on chemotherapy treatment.

(G) 1×10^6 mouse mammary tumor 4T1 cells were injected into the mammary gland of Balb/c mice. After the tumor size reached 100 mm^3 , mice were treated with cisplatin, BAPN or combination. Tumor weight of mice with subcutaneous injection at day 28 after treatment. The Bliss Independence model of additivity indicates an additive effect of the drug combination for a synergistic effect for BAPN and cisplatin. **: $p < 0.01$.

(H) Tumor growth was measured at the indicated times after treatment. $n = 5$ for each group. (**: $p < 0.01$, by two-way ANOVA.)

(I) Tumor images from (G).

(J) Protein extraction of tumor from (G) were run on SDS-PAGE gel and probed with indicated antibodies.

Figure S2

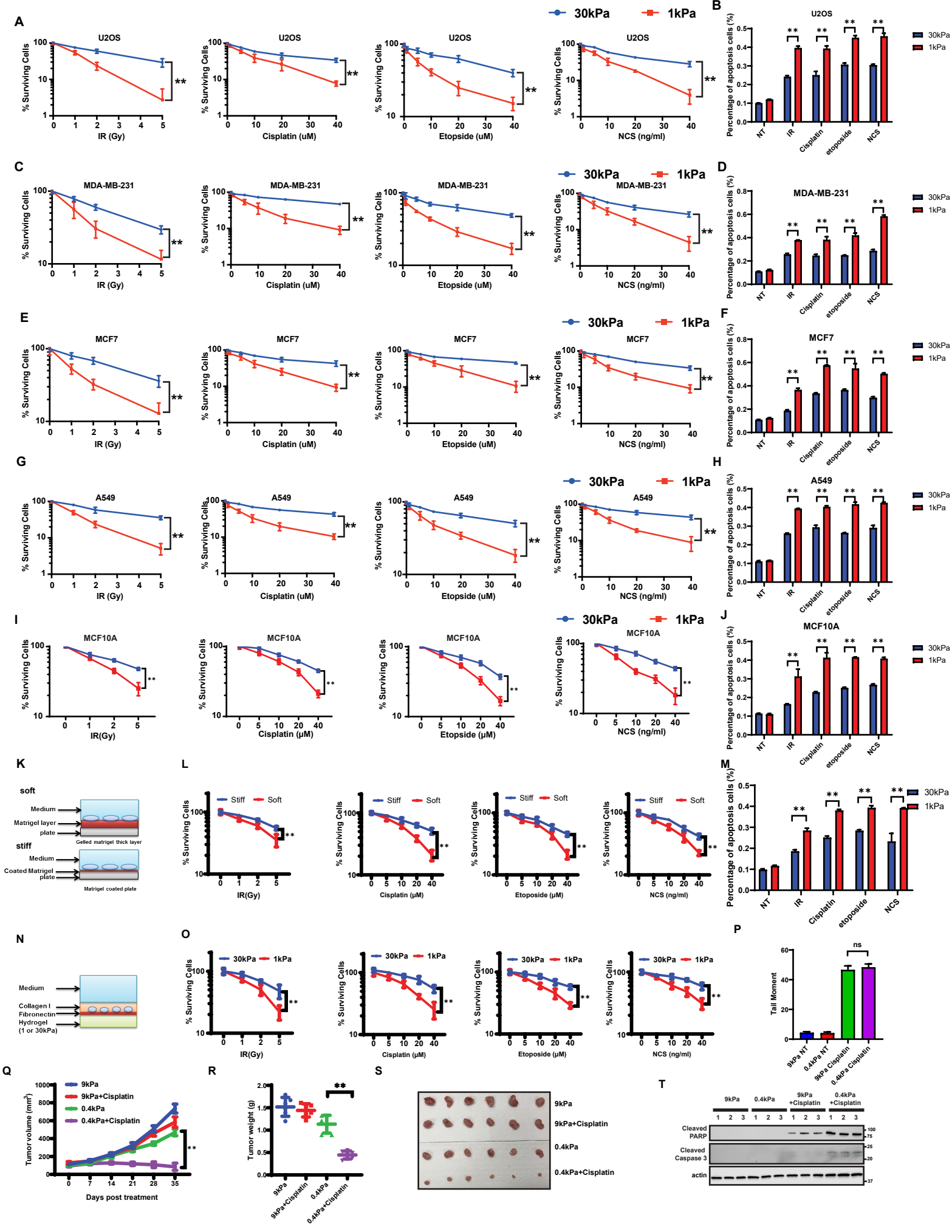


Fig.S2 Low stiffness impairs DSB repair and increases cellular sensitivity to genotoxic agents.

(A).U2OS cells were plated on low (1 kPa) and high (30 kPa) stiff hydrogel coated with fibronectin. Cells were treated with indicated genotoxic agents. Colonogenic assays were performed to detect cell survival on different ECM.

(B).U2OS cells were plated on low (1 kPa) and high (30 kPa) stiff hydrogel coated with fibronectin. Cells were treated with indicated genotoxic agents (10 Gy IR, 10 μ M cisplatin, 10 μ M etoposide, 10 ng/ml NCS). Cells were trypsinized after 48h and cellular apoptosis was detected by Annexin V and PI staining. Error bars represent SD of the mean for 3 replicate samples analyzed in one experiment.

(C). MDA-MB-231 cells were plated on low (1 kPa) and high (30 kPa) stiff hydrogel coated with fibronectin. Cells were treated with indicated genotoxic agents. Colonogenic assays were performed to detect cell survival on different ECM.

(D). MDA-MB-231 cells were plated on low (1 kPa) and high (30 kPa) stiff hydrogel coated with fibronectin. Cells were treated with indicated genotoxic agents (10 Gy IR, 10 μ M cisplatin, 10 μ M etoposide, 10 ng/ml NCS). Cells were trypsinized after 48h and cellular apoptosis was detected by Annexin V and PI staining. Error bars represent SD of the mean for 3 replicate samples analyzed in one experiment.

(E). MCF7 cells were plated on low (1 kPa) and high (30 kPa) stiff hydrogel coated with fibronectin. Cells were treated with indicated genotoxic agents. Colonogenic assays were performed to detect cell survival on different ECM.

(F). MCF7 cells were plated on low (1 kPa) and high (30 kPa) stiff hydrogel coated with fibronectin. Cells were treated with indicated genotoxic agents (10 Gy IR, 10 μ M cisplatin, 10 μ M etoposide, 10 ng/ml NCS). Cells were trypsinized after 48h and cellular apoptosis was detected by Annexin V and PI staining. Error bars represent SD of the mean for 3 replicate samples analyzed in one experiment.

(G). A549 cells were plated on low (1 kPa) and high (30 kPa) stiff hydrogel coated with fibronectin. Cells were treated with indicated genotoxic agents. Colonogenic assays were performed to detect cell survival on different ECM.

(H). A549 cells were plated on low (1 kPa) and high (30 kPa) stiff hydrogel coated with fibronectin. Cells were treated with indicated genotoxic agents (10 Gy IR, 10 μ M cisplatin, 10 μ M etoposide, 10 ng/ml NCS). Cells were trypsinized after 48h and cellular apoptosis was detected by Annexin V and PI staining. Error bars represent SD of the mean for 3 replicate samples analyzed in one experiment.

(I).MCF10A cells were plated on low (1 kPa) and high (30 kPa) stiff hydrogel coated with fibronectin. Cells were treated with indicated genotoxic agents. Colonogenic assays were performed to detect cell survival on different ECM.

(J).MCF10A cells were plated on low (1 kPa) and high (30 kPa) stiff hydrogel coated with fibronectin. Cells were treated with indicated genotoxic agents (10 Gy IR, 10 μ M cisplatin, 10 μ M etoposide, 10 ng/ml NCS). Cells were trypsinized after 48h and cellular apoptosis was detected by Annexin V and PI staining. Error bars represent SD of the mean for 3 replicate samples analyzed in one experiment.

(K) Model of cell culture on Matrigel coated plates (stiff) and Matrigel thick layer (soft).

(L) HEK293 cells were plated on Matrigel coated plates (stiff) and Matrigel thick layer (soft). Cells were treated with indicated doses of genotoxic agents. Colony formation assays were performed to detect cell survival on different ECM. Data are presented as mean \pm S.D., n = 3 biologically independent samples. (**: p < 0.01)

(M) HEK293 cells were plated on Matrigel coated plates (stiff) and Matrigel thick layer (soft). Cells were treated with indicated genotoxic agents (10 Gy IR, 10 μ M cisplatin, 10 μ M etoposide, 10 ng/ml NCS). Cells were trypsinized after 48h and cellular apoptosis was detected by Annexin V and PI staining. Error bars represent SD of the mean for 3 replicate samples analyzed in one experiment.

(N) Model of 3D cell culture on stiff (30 kPa) and soft (1 kPa) hydrogels.

(O) HEK293 cells were grown on stiff (30 kPa) and soft (1 kPa) hydrogels and overlaid with Collagen I. Cells were treated with indicated doses of genotoxic agents. Colony formation assays were performed to detect cell survival on different ECM. Data are presented as mean \pm S.D., n = 3 biologically independent samples. (**: p < 0.01)

(P) 5×10^6 MDA-MB-231 cells were embedded in 200 μ l of 0.4 or 9.0 kPa hyaluronan-based gel and were subcutaneously injected into nude mice. Mice were treated with or without cisplatin at 1 mg/kg for 6h. Cells from tumor were trypsinized and harvested for neutral comet assay.

(Q) 5×10^6 MDA-MB-231 cells were embedded in 200 μ l of 0.4 or 9.0 kPa hyaluronan-based gel and were subcutaneously injected into nude mice. Mice were treated with or without cisplatin at 1 mg/kg/day. Tumor growth was measured at the indicated times after treatment. n = 6 for each group. (**: p < 0.01, by two-way ANOVA.)

(R) Tumor weight of mice with subcutaneous injection as described in (I) at day 35 after treatment. **: p < 0.01, by two-way ANOVA.

(S) Images of tumors from (R).

(T) Protein extraction of tumor from (R) were run on SDS-PAGE gel and probed with indicated antibodies.

Figure S3

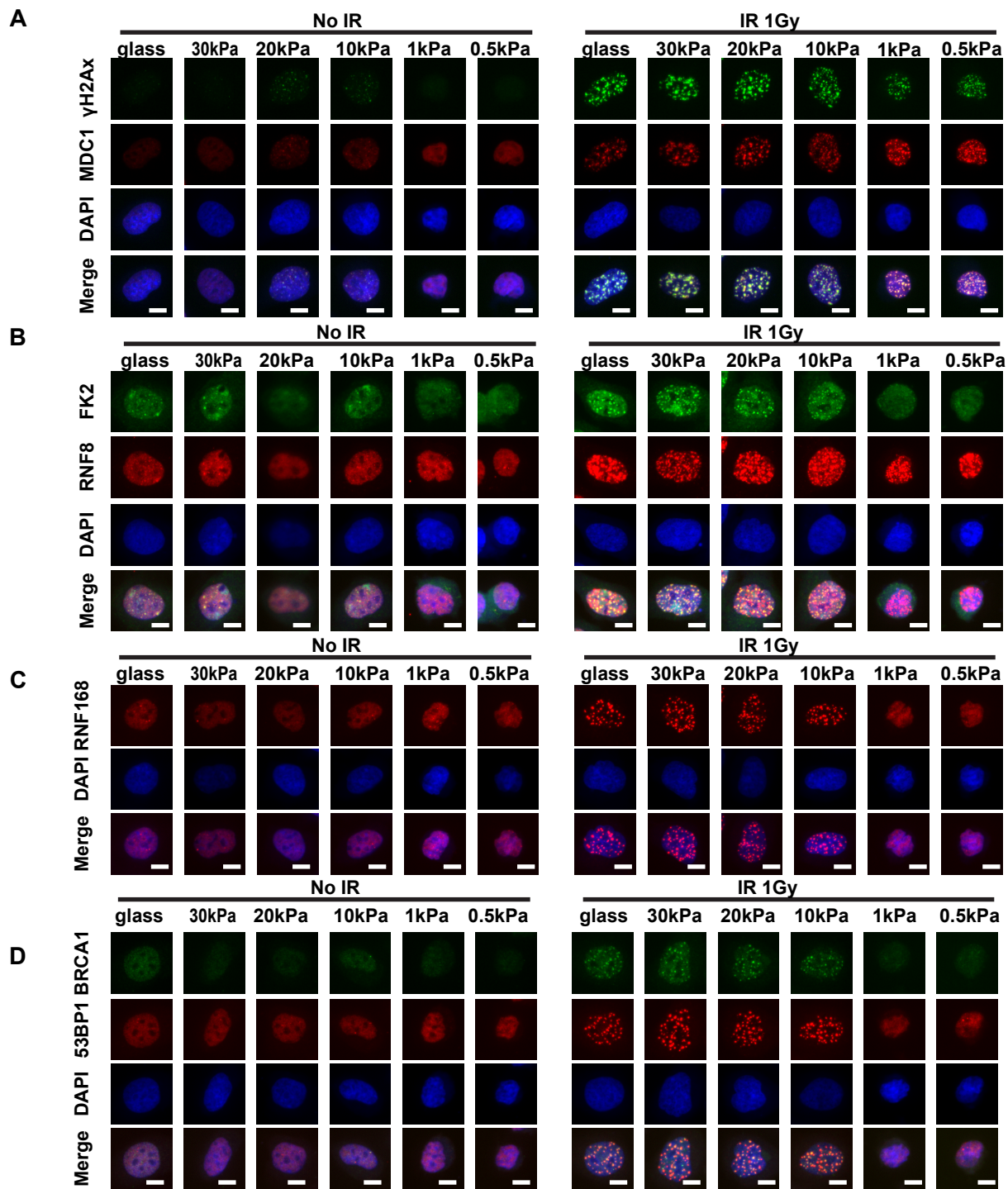


Fig.S3 Low stiffness inhibits DSB repair at the level of RNF8 in the DSB repair pathway.

(A-D) HEK293 cells were grown on fibronectin coated hydrogels of different stiffness for 24 hours. Cells were fixed 1 hour after irradiation (1 Gy) and stained with anti- γ -H2AX and MDC1 (A), RNF8 and FK2 (B), 53BP1 and BRCA1 (D) antibodies. For RNF168 (C), HEK293 cells expressing mCherry-RNF168 were plated on fibronectin coated hydrogels of different stiffness. Cells were fixed 1 hour after irradiation (1 Gy) and RNF168 foci were visualized with mCherry. Representative images showing IR induced foci after 1Gy irradiation. Scale bar, 10 μ M

Figure S4

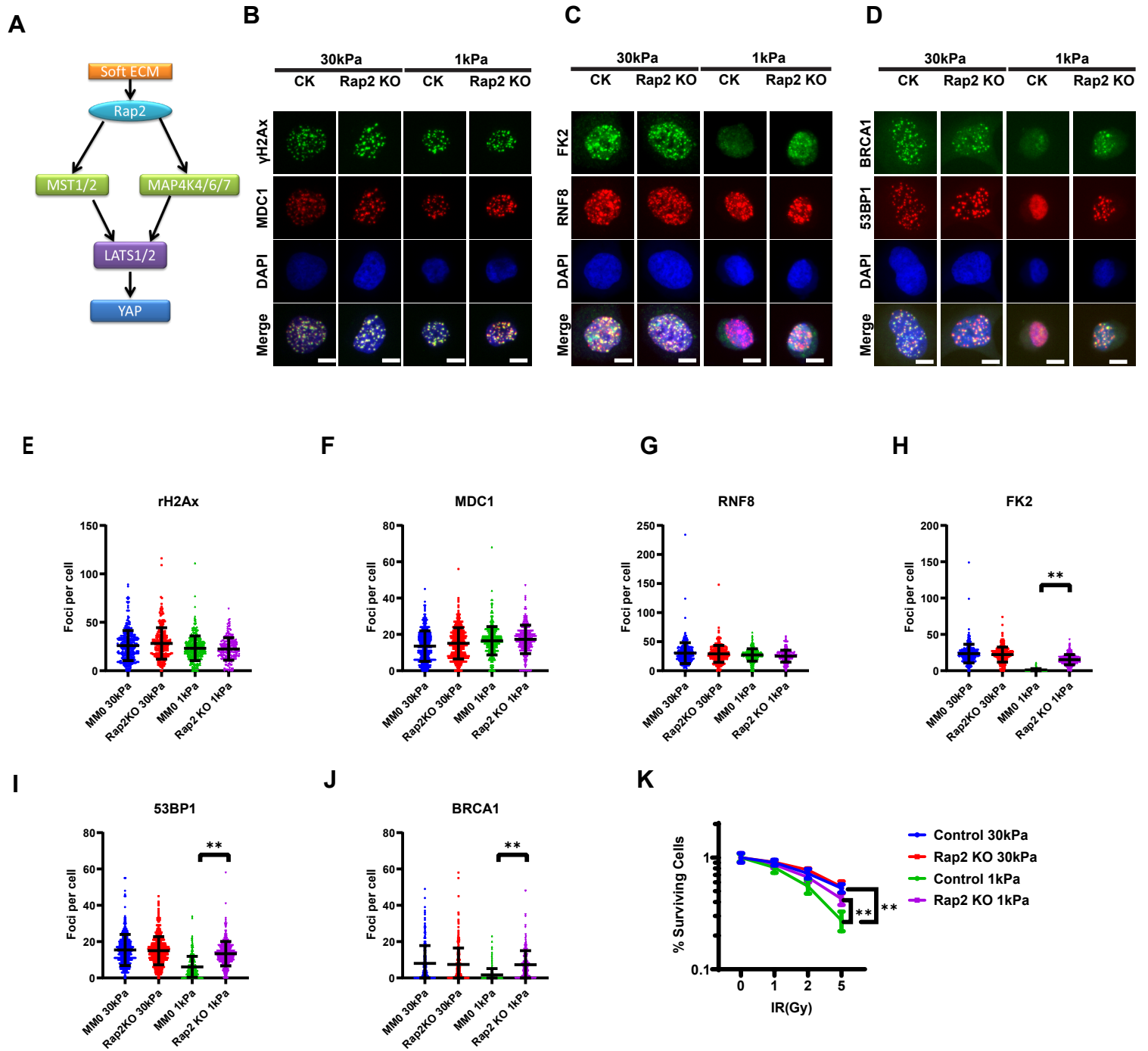


Fig.S4 Inhibition of DSB repair by low stiffness is dependent on Rap2.

(A) A model showing the role of Rap2 in mechanotransduction.

(B to D) Control (CK) and Rap2 knockout (Rap2KO) HEK293 cells were grown on soft (1 kPa) and stiff (30 kPa) fibronectin coated hydrogels. Cells were fixed 1 hour after irradiation (1Gy) and stained with anti- γ -H2AX and MDC1 (B), RNF8 and FK2 (C), 53BP1 and BRCA1 (D) antibodies. Scale bar, 10 μ M.

(E to J) Quantification of (B to D) is described in Methods. Data are presented as mean \pm S.D., n = 3 biologically independent samples. (**: p < 0.01)

(K) Rap2 is required for regulation of stiffness-induced radiation sensitivity. Colony formation assays were performed to examine radio-sensitivity of wild type (Control) and Rap2 knockout (Rap2KO) HEK293 cells on soft (1 kPa) and stiff (30 kPa) fibronectin coated hydrogels. Data are presented as mean \pm S.D., n = 3 biologically independent samples. (**: p < 0.01)

Figure S5

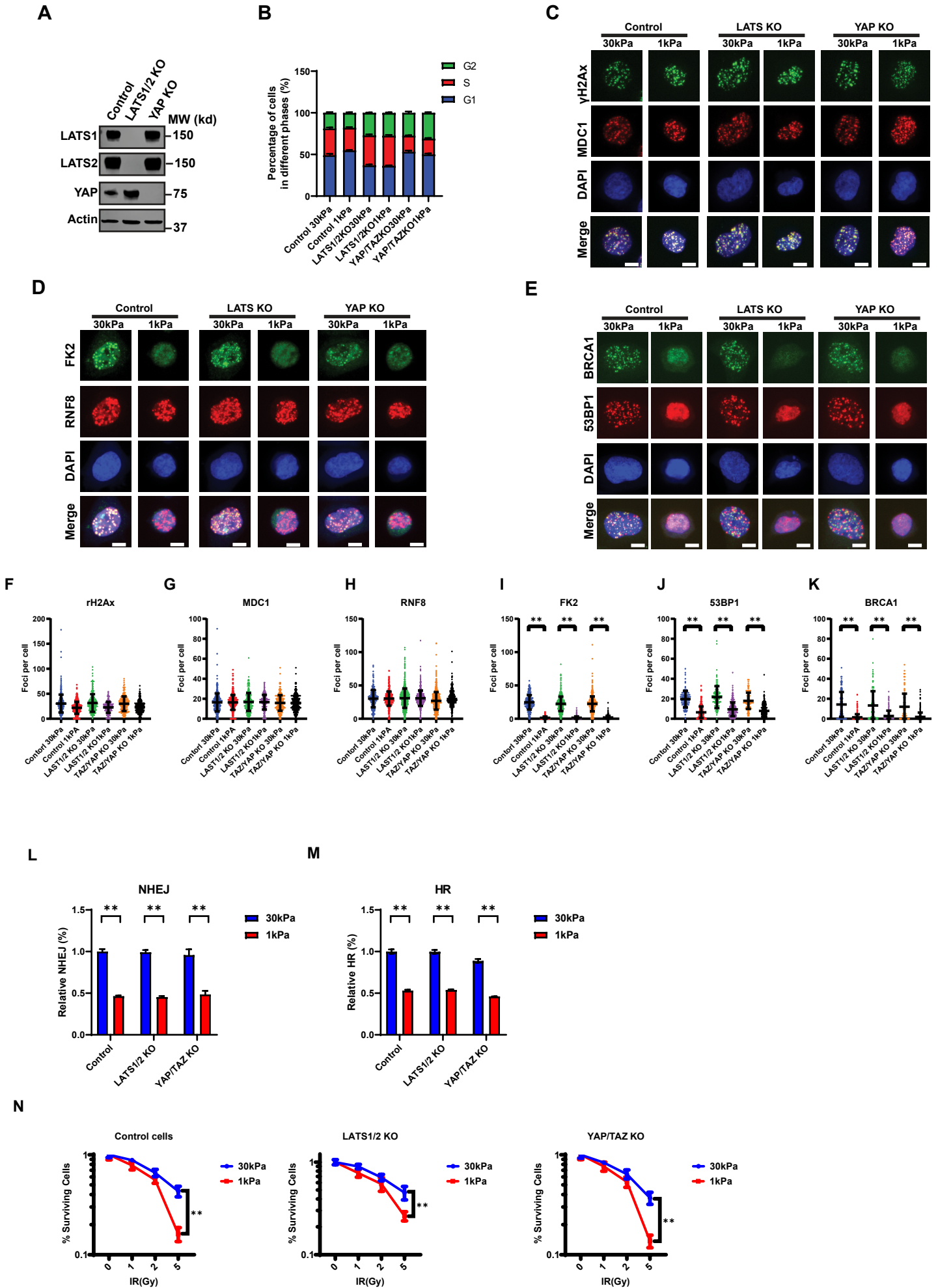


Fig.S5 Inhibition of DSB repair by low stiffness is independent LATS/YAP.

(A) Western blots showing the expression levels of LATS1/2 and YAP in control, LATS1/2 knockout (LATS1/2 KO) and YAP/TAZ knockout (YAP/TAZ KO) HEK293 cells.

(B) Control (MM0), LATS1/2 KO (LATS KO) and YAP/TAZ KO (YAP KO) cells were grown on soft (1 kPa) and stiff (30 kPa) fibronectin coated hydrogels for 24 hours. Cell cycle distribution was detected by flow cytometry.

(C to E) Control (MM0), LATS1/2 KO (LATS KO) and YAP/TAZ KO (YAP/TAZ KO) cells were grown on soft (1 kPa) and stiff (30 kPa) fibronectin coated hydrogels for 24 hours. Cells were fixed 1 hour after irradiation and stained with indicated antibodies. Scale bar, 10 μ M.

(F to K) Quantification of (C to E) is described in Methods.

(L and M) Control, LATS1/2 KO and YAP/TAZ KO cells were grown on soft (1 kPa) and stiff (30 kPa) fibronectin coated hydrogels. Effect of ECM stiffness on the efficiency of NHEJ (L) and HR (M) in indicated cells was analyzed by flow cytometry.

(N) LATS1/2 kinases and YAP/TAZ are not required for stiffness-induced regulation of radiation sensitivity. Colony formation assays were performed to examine survival of Control, LATS1/2 KO and YAP/TAZ KO cells on soft (1 kPa) and stiff (30 kPa) fibronectin coated hydrogels.

Figure S6

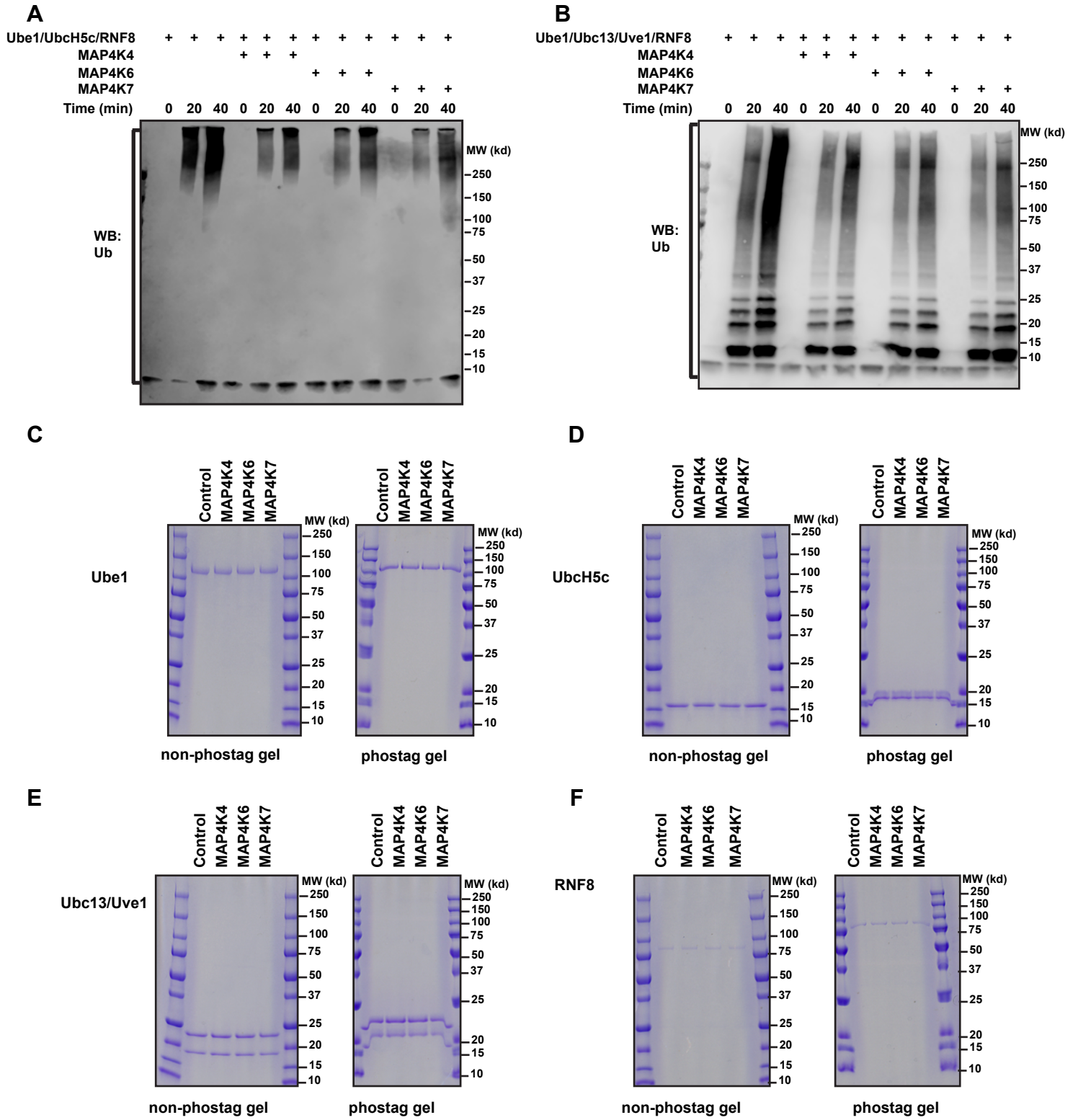


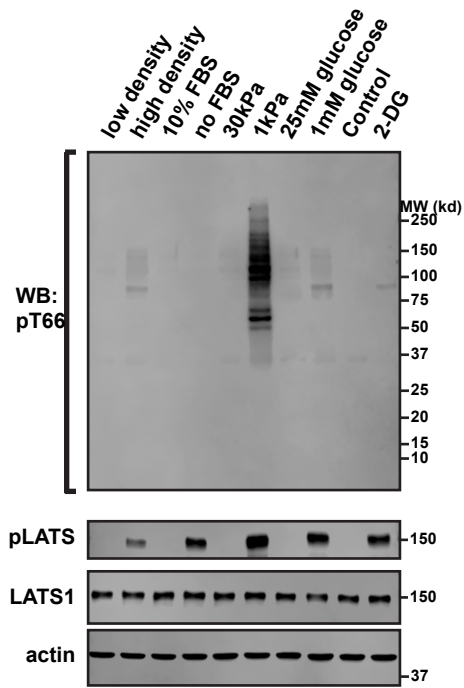
Fig.S6 MAP4K4/6/7 kinases directly inhibit RNF8 mediated ubiquitin chain formation *in vitro*.

(A and B) MAP4K4/6/7 kinases impair RNF8 mediated ubiquitin chain formation *in vitro*. The assembly of ubiquitin chains was determined at 30°C in the presence of Ube1, UbcH5c (A) or Ubc13/Uve1 (B) and RNF8 with indicated kinases. Samples were taken at the indicated time points, and polyubiquitin chains were detected by immunoblotting with an anti-Ub antibody.

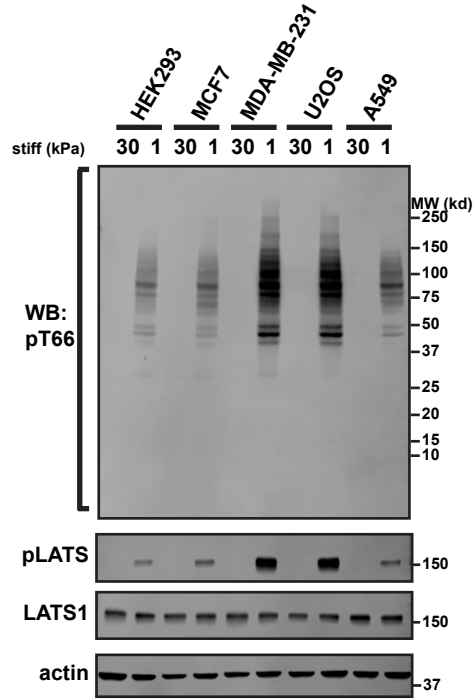
(C to F) MAP4K4/6/7 kinases do not phosphorylate Ube1, UbcH5c, Ubc13/Uve1 or RNF8 *in vitro*. An *in vitro* kinase assay was performed at 30°C for 1hour in the presence of Ube1(C), UbcH5c (D), Ubc13/Uve1 (E) or RNF8 (F) and indicated kinases. Samples were run on non-phos-tag or phos-tag PAGE and the gels were stained with Coomassie Brilliant Blue (CBB).

Figure S7

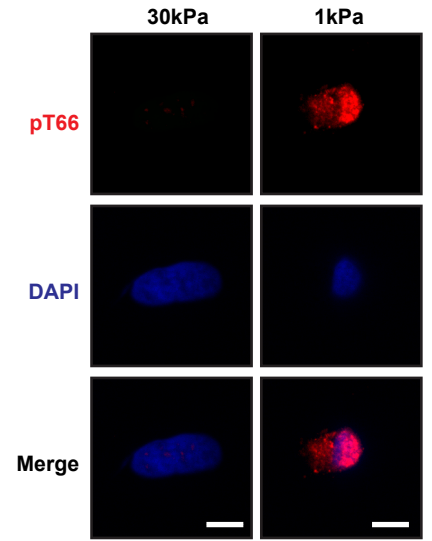
A



B



C



D

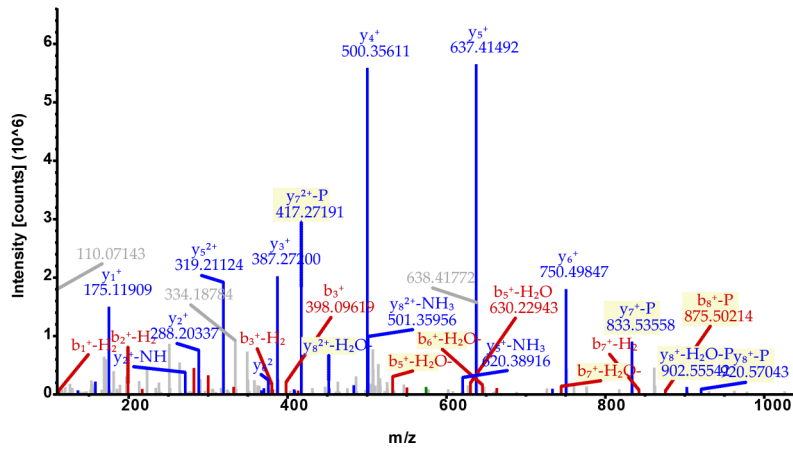


Fig.S7 Phosphorylation of Ub is regulated by stiffness in cells.

(A) HEK293 cells were treated with indicated conditions and cell lysates were blotted with indicated antibodies.

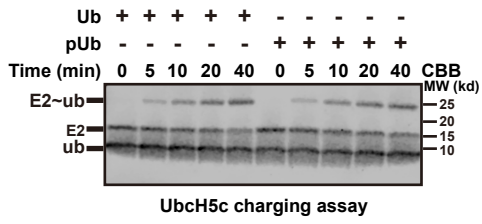
(B) Different cells were grown on soft (1 kPa) and stiff (30 kPa) fibronectin coated hydrogels. Cell lysates were blotted with indicated antibodies.

(C) HEK293 cells were grown on soft (1 kPa) and stiff (30 kPa) fibronectin coated hydrogels for 24 hours. Cell were fixed and stained with anti-pT66 antibody. Scale bar, 10 μ M.

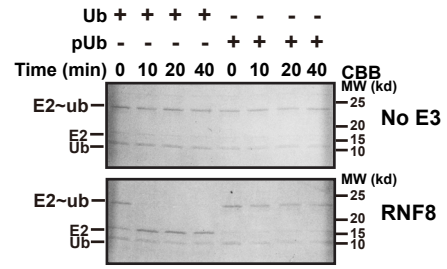
(D) Lysates from HEK293 cells grown on soft hydrogel (1 kPa) was trypsinized and subjected to liquid chromatography tandem mass spectrometry (LC-MS/MS) analysis. One peptide (ES^pTLHLVLR) corresponding to ubiquitin Thr66 phosphorylation was identified.

Figure S8

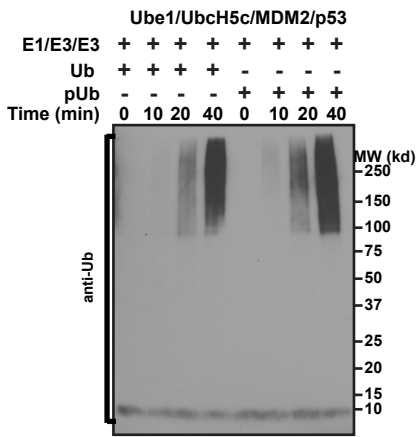
A



B



C



D

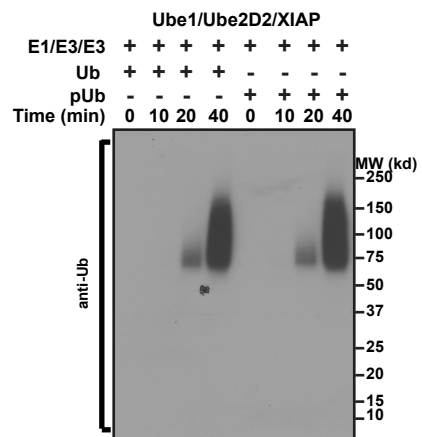


Fig.S8 Phosphorylation of ubiquitin blocks RNF8 mediated ubiquitin conjugation *in vitro*.

(A) E1-mediated UbcH5c charging is not affected by ubiquitin T66 phosphorylation. E1-mediated charging of E2 enzyme by Ub and phos-Ub was examined in a time-course analysis. Reactions were stopped with 2 × non-reducing buffer and processed on non-reducing SDS-PAGE. “Ub~” refers to generation of a thioester with E2 enzyme.

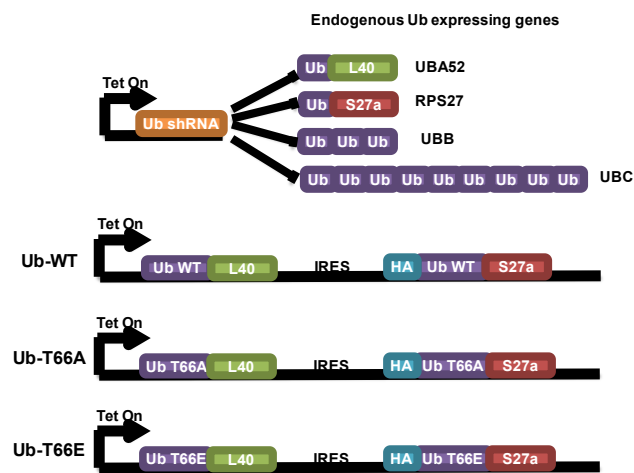
(B) RNF8 mediated E2 discharging is blocked by phosphorylation of Ub. UbcH5c charged with ubiquitin (UbcH5c~Ub) was mixed with Ub-His₆ or phosUb-His₆ in E2 discharging buffer. RNF8 or MDM2 were included as indicated and reaction were performed at 37°C for the indicated times. Reactions were stopped with 2 × non-reducing buffer and processed on non-reducing SDS-PAGE.

(C) Ubiquitin T66 phosphorylation does not affect MDM2 mediated ubiquitin chain formation. Phospho-Ub was prepared and purified as described in Methods. The assembly of ubiquitin chains was determined at 30°C in the presence of Ube1, UbcH5c, MDM2, p53 and indicated Ub variants. Samples were taken at the indicated time points, and polyubiquitin chains were detected by immunoblotting with an anti-Ub antibody.

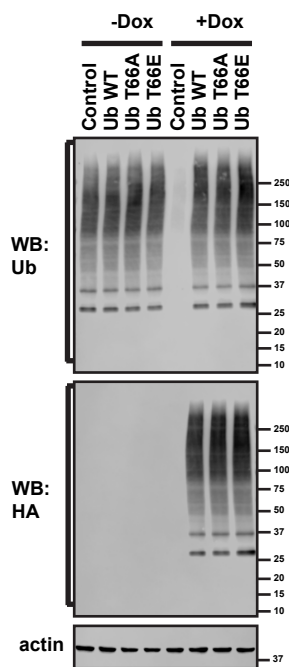
(D) Ubiquitin T66 phosphorylation does not affect XIAP mediated ubiquitin chain formation. The assembly of ubiquitin chains was determined at 30°C in the presence of Ube1, Ube2D2, XIAP and indicated Ub variants. Samples were taken at the indicated time points, and polyubiquitin chains were detected by immunoblotting with an anti-Ub antibody.

Figure S9

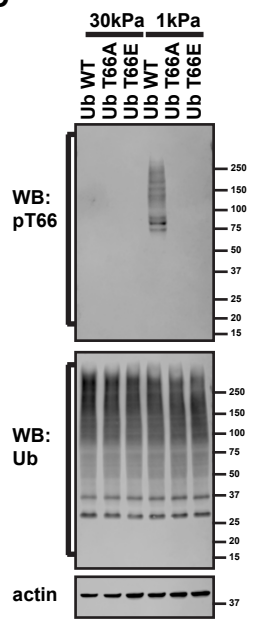
A



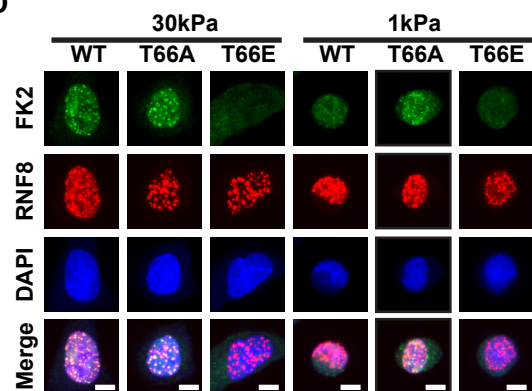
B



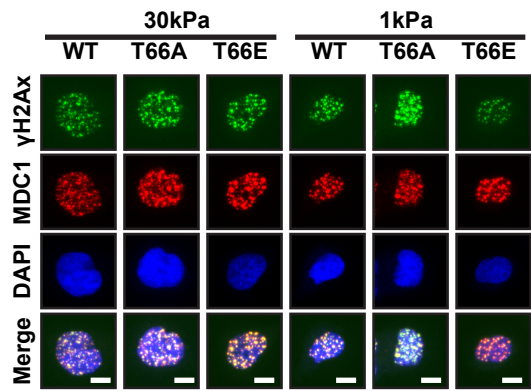
C



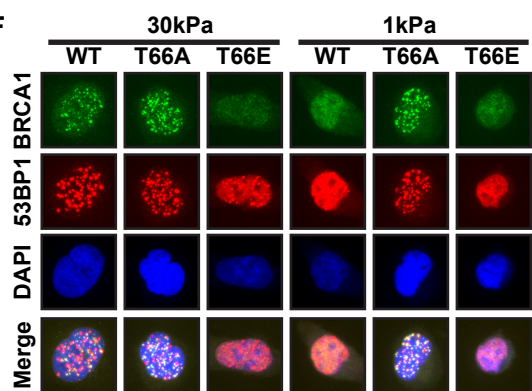
D



E



F



G

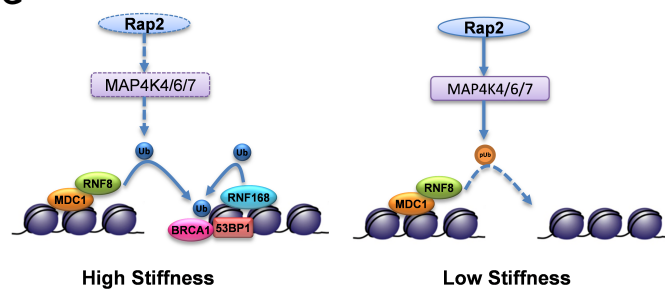


Fig.S9 Phosphorylation of ubiquitin mediates DNA repair blockage in cells at low stiffness.

(A) Schematic of the ubiquitin-replacement system used here to replace endogenous Ub with WT Ub, Ub T66A and Ub T66E mutants.

(b) Validation of ubiquitin-replacement HEK293 cells. The indicated cells induced with 2 μ M Dox for 72 hours. The levels of HA-Ub, Ub T66A and Ub T66E were measured by immunoblotting. Actin was used as a loading control.

(C) Replacement of ubiquitin with phospho-deficient ubiquitin mutant T66A or T66E blocks ubiquitin phosphorylation at low stiffness. Replacement of ubiquitin was induced by 2 μ M Dox for 48h. Cells were then plated on low (1 kPa) or high (30 kPa) stiff hydrogel coated with fibronectin and cultured for 24h. The level of ubiquitin phosphorylation was detected with indicated antibodies.

(D to F) Replacement of ubiquitin with phospho-deficient ubiquitin mutant T66A restores FK2, 53BP1 and BRCA1 foci at low stiffness. Ubiquitin-replacement HEK293 cells expressing wild-type (WT), T66A and T66E ubiquitin were grown on soft (1 kPa) and stiff (30 kPa) fibronectin coated hydrogels. Cells were fixed 1 hour after irradiation (1 Gy) and stained with anti- γ -H2AX and MDC1 (D), RNF8 and FK2 (E), 53BP1 and BRCA1 (F) antibodies. Representative images showing IR induced foci after 1 Gy irradiation. Scale bar, 10 μ M.

(G) A working model for this study.